Astronomy Letters, Vol. 23, No. 1, 1997, pp. 64–70. Translated from Pis'ma v Astronomicheskii Zhurnal, Vol. 23, No. 1–2, 1997, pp. 83–89.

The Fine Structure of Compact Radio Sources from Geodetic Data

E. A. Airapetyan[1] and L. I. Matveenko[2]

[1] *Institute of Applied Astronomy, Russian Academy of Sciences, St. Petersburg, Russia*
[2] *Space Research Institute, Russian Academy of Sciences, Profsoyuznaya ul. 84/32, Moscow, 117810 Russia*

Received July 8, 1996

Abstract—Geodetic VLBI observations at a frequency of 8.4 GHz with an angular resolution of 0.25 mas are used to determine the fine structure of a number of compact extragalactic radio sources with active nuclei. The brightness temperature of compact components is $T_b \leq 10^{12}$ K.

1. INTRODUCTION

Very long baseline interferometry (VLBI) is currently widely used to address astrophysical and astrometrical–geodynamical problems (Matveenko *et al.* 1965). The measured quantities in this technique are the complex correlation coefficients, group delays, and fringe frequencies of correlations between the recorded signals. Images of radio sources are constructed using complex correlation coefficients, while the solution of astrometrical problems is based on measuring group delays and fringe frequencies (Matveenko *et al.* 1983). The construction of astronomical images requires the maximum possible *UV*-plane coverage, i.e., the maximum possible continuity of the Fourier spatial frequencies for the transform of the studied object. In astrometry, sparse observations—gaps in the spatial frequency spectrum—are admissible.

Astrometrical–geodynamical studies are based on measurements of reference radio sources. Compact extragalactic radio sources are used as these reference sources; these objects have active nuclei. Although compact, these objects are not so small that we can completely ignore their sizes. The activity in their nuclei leads to changes in their visible structure and their radio brightness distribution; this unavoidably causes changes in the center of gravity of the images and, accordingly, changes in the reference coordinates. Systematic astrometric observations may be used to study the structures of these reference objects, investigate their physical nature and evolution (Charlot 1990), and determine the variations in their coordinates.

Geodetic VLBI measurements are regularly conducted on a global radio interferometry network simultaneously at frequencies of 8.4 and 2.3 GHz; one element of this network is the Simeiz VLBI station (Clark *et al.* 1995). The geodetic observational data bank at Goddard has "public domain" status; i.e., the data are accessible to a wide circle of researchers. We have used such data to construct images for a number of reference objects which are considered below.

CONSTRUCTION OF THE IMAGES

Geodetic VLBI observations are regularly conducted on the radiotelescopes indicated in Tab. 1. This table shows the telescope diameters, source effective flux Densities (SEFD), and system noise temperatures, expressed in terms of the effective area of the antenna in flux units. The angular resolution, i.e., the width of the interference fringes, of this network reaches 0.6 mas at 8.4 GHz.

Geodetic observations are usually done using a "snapshot" method, in which a group of sources is observed sequentially, with each object observed for 20 min, in order to obtain a large overlap in hour angles. This leads to large gaps in the *UV*-plane cover-

Table 1. Antenna parameters

Antenna	Diameter, m	SEFD, Jy
DSS65, Spain	34	190
Noto, Italy	32	750
Medicina, Italy	32	340
Matera, Italy	20	3200
Weitzel, Bavaria	20	800
Onsala, Sweden	20	1925
Simeiz, Ukraine	22	1000
Gilcreek, USA	26	750
Koki, USA	20	850
Green Bank, USA	26	720
Fortaleza, Brazil	14	3200
DSS15, USA	34	200
Kashima, Japan	26	2100
Westford, USA	18	1400

1063-7737/97/2301-0064$10.00

age for each of the measured sources. Figure 1 shows the mutual visibility between pairs of antennas for one of the sources, 1803+784. The observations are conducted on universal (not stellar) time, so that it is possible to expand the coverage of the *UV* plane by joining data from several sessions. The dynamic range of measurements using these data is on average 100 : 1.

We synthesized the images presented here from the correlation coefficient data using the CalTech VLBI package (Pearson 1991). We used the SEFD coefficients for 8.4 GHz observations in the zenith direction given in Table 1 (Shaffer *et al.* 1987).

Various algorithms are used to construct the radio brightness distributions of sources from correlated flux measurements. The most modern of these is hybrid mapping, which constructs radio images taking into account the closure phases of the data (the relative phase tie of spatial harmonics). This method also allows for self-calibration of the correlated fluxes using the closure amplitudes, which determines refined values for the SEFD coefficients for each moment of time. The image of the object, whose Fourier transform corresponds to the measured correlated fluxes, is then constructed by the program "FT" using a least-squares method. This iterative fitting process continues until the maximum agreement is reached between the correlated fluxes for the original data and calculated for the model.

The resulting image ("dirty map") is significantly distorted due to the incomplete coverage of the *UV* plane, and it is necessary to correct it for the antenna beam. We may synthesize the antenna beam using the known *UV* plane coverage. The program "CLEAN" makes this correction—it "cleans" the "dirty" map. The resulting images and widths of the antenna beams at the half-power level are shown in Fig. 2.

RESULTS

We present maps for some objects observed as part of the geodetic VLBI program at frequency 8.4 GHz. Table 2 gives a list of the objects we have studied, their identifications, redshifts z, distances R in Mpc (H is assumed to be 100 km s^{-1} Mpc^{-1}), the linear sizes L in pc corresponding to 1 mas, radio flux density at 8.4 GHz F_0 in Jy, flux density in the antenna beam in Jy/beam, and the brightness temperature T_b in K.

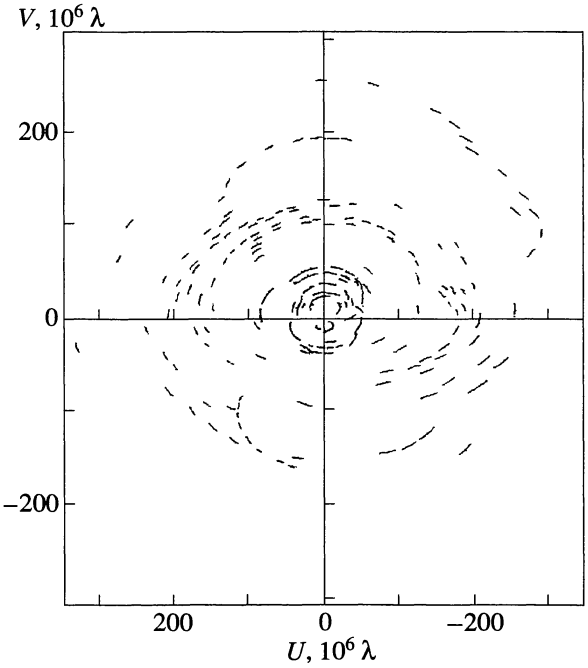

Fig. 1. *UV* plane coverage for the source 1803+784, expressed in units of 10^6 wavelengths.

We can see from this table that these sources are quasars, BL Lacertae objects, and blazars, i.e., objects with active nuclei. We will examine the resulting brightness distributions for these objects.

Object 0059+581. Reference to this source was first made by Becker *et al.* (1991). It does not have an optical identification, and therefore its redshift and distance are unknown. Our map of its radio brightness distribution at 8.4 GHz, with resolution 0.25 mas, is shown in Fig. 2.1a. This object has a jet in structural position angle PA = −150°. The size of the core is 0.25 mas, and its brightness temperature is $T_b = 0.9 \times 10^{12}$ K. The brightness distribution along the jet axis is shown in Fig. 2.1b.

Object 0229+131. This quasar has a complex structure which consists of a compact core (the bright component) and two components symmetrically located relative to it. It is possible that the core is actually one of the end components, and that the other two compo-

Table 2. Reference source data

Name	Type of object	Z	R, Mpc	L, pc/mas	F_0, Jy	F, Jy/beam	T_b, 10^{12} K
0059+581	–	–	–	–	2.75	2.35	0.9
0229+131	QSO	2.059	7860	4.07	0.83	0.35	0.2
0528+134	Blazar	2.060	7864	4.06	3.38	2.29	0.7
1308+326	BL Lac	0.996	3499	4.26	3.33	2.13	1.0
1803+784	BL Lac	0.680	2303	3.95	2.25	1.18	0.1
2145+067	Blazar	0.990	3476	4.25	5.22	3.73	1.4
2234+282	QSO	0.795	2731	4.11	0.90	0.49	0.1

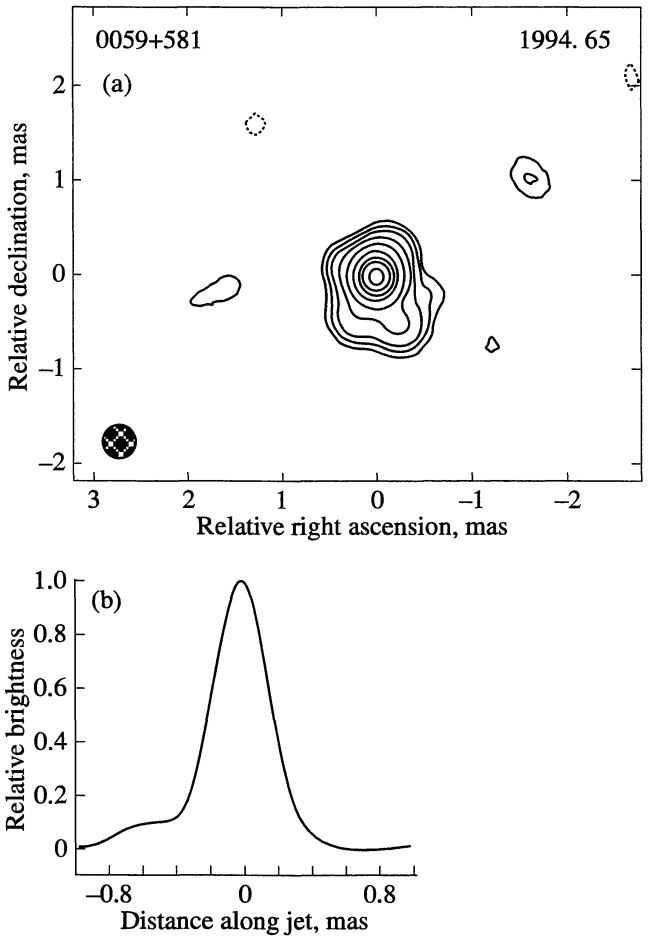

Fig. 2.1. (a) Brightness distribution for 0059+581 at 3.6 cm. The width of the synthesized antenna beam at the 3-dB level is shown in the lower left corner. The isophotes are drawn for levels 1, 2, 4, 8, 16, 32, 50, 64, and 85% of the maximum value. The resolution is 0.35 × 0.35 mas, and the map peak is 2.04 Jy/beam. (b) Brightness distribution along the jet, in position angle PA = –200°. The maximum corresponds to 2.04 Jy/beam.

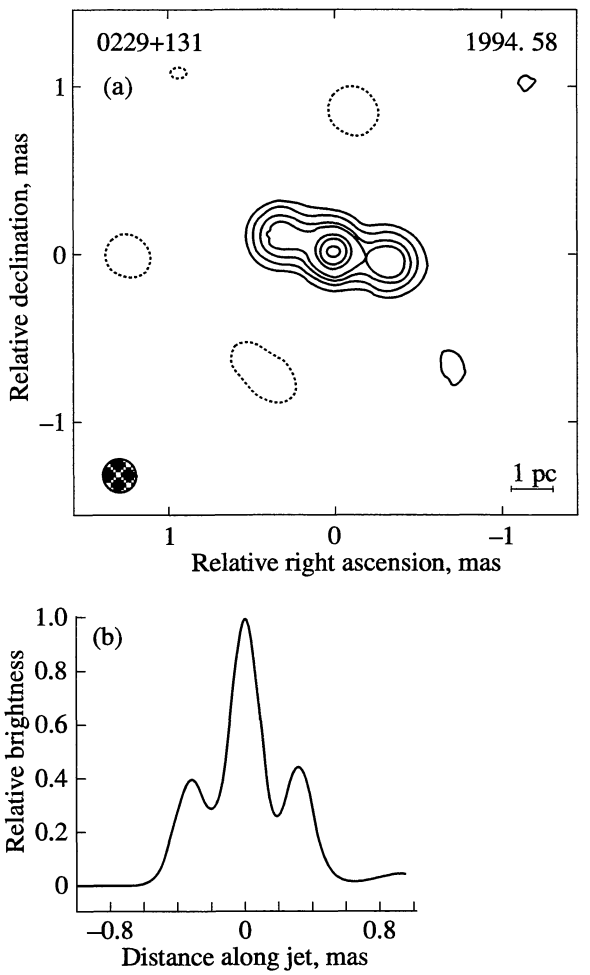

Fig. 2.2. (a) 0229+131. Same as in Fig. 2.1 a. The resolution is 0.20 × 0.20 mas, and the map peak is 0.35 Jy/beam. (b) Brightness distribution along the jet, in position angle PA = –70°. The maximum is 0.35 Jy/beam.

nents form a jet (Fig. 2.2a). The size of the compact components is 0.2 mas, or 0.8 pc. The brightness temperature of the central component is $T_b = 0.2 \times 10^{12}$ K, while the brightness temperature for the other two components is $T_b = 0.07 \times 10^{12}$. Figure 2.2b shows the brightness distribution along the direction of the structure (PA = 70°). The components are separated by a distance 0.35 mas, or 1.4 pc.

These results refine the maps obtained at 8.4 GHz by Charlot (1990). The angular resolution in those images was lower, and showed only that the object was extended along PA = 45°.

Object 0528+134. This blazar is among the strongest gamma sources, and a black hole candidate (Schonfelder 1994). Previous measurements at 8.4 and 2.3 GHz revealed the source to be slightly extended along position angle –140° (Charlot 1990). In our images, we observe a jet in PA = 50° (Fig. 2.3a). This jet is curved, possibly indicating spiral structure. The size of the core is 0.27 mas, or 1.1 pc, and its brightness temperature is $T_b = 0.7 \times 10^{12}$ K. Figure 2.3b shows the brightness distribution along the jet.

Object 1308+326. In 5-Ghz VLBI observations of this BL Lacertae object (Gabuzda *et al.* 1993), it is possible to distinguish a core and extended region with size 5 mas (21 pc) toward the west. Gabuzda *et al.* (1993) propose that this object is a quasar with very weak emission lines. The core has a simple structure with size 1.3 × 0.6 mas, oriented along PA = –30° (Zensus *et al.* 1984).

According to our data, the central source at 8.4 GHz includes a bright core (0.22 mas) and a jet structure extending along PA = –25° (Fig. 2.4a). The brightness

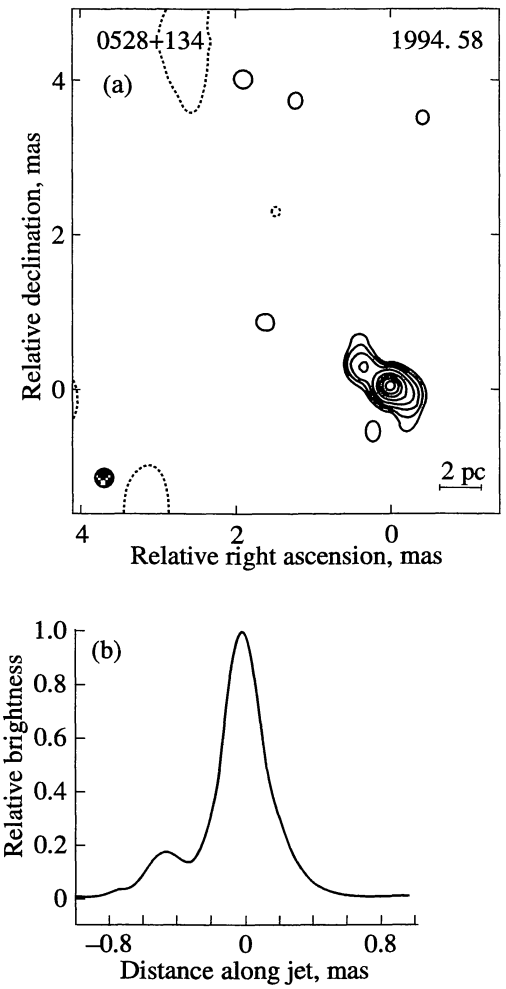

Fig. 2.3. (a) 0528+134. Same as in Fig. 2.1 a. The resolution is 0.25 × 0.25 mas, and the map peak is 2.3 Jy/beam. (b) Brightness distribution along the jet, in position angle PA = 50°. The maximum is 2.3 Jy/beam.

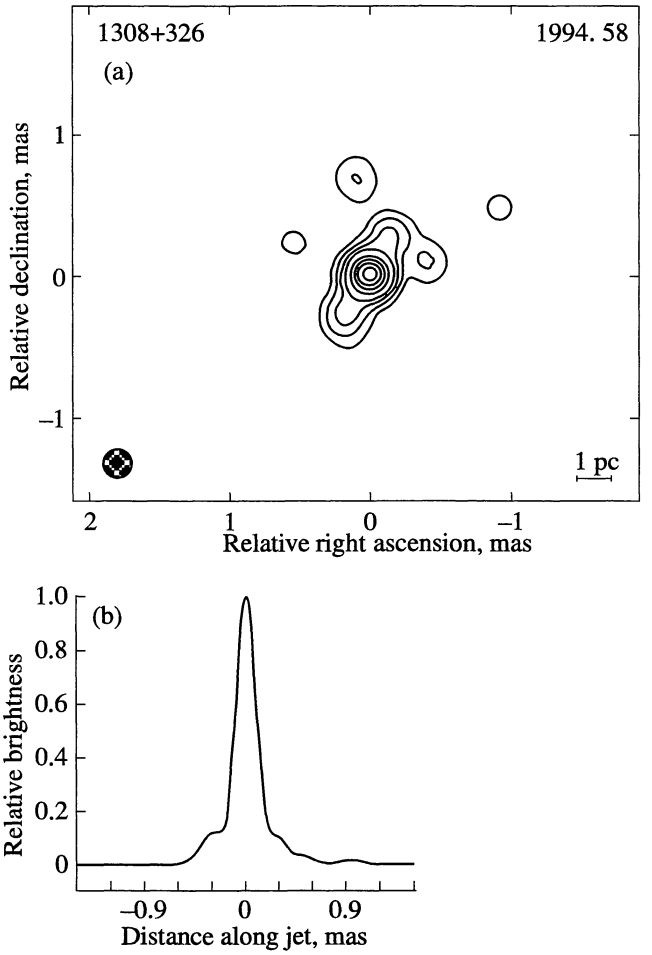

Fig. 2.4. (a) 1308+326. Same as in Fig. 2.1 a. The resolution is 0.20 × 0.20 mas, and the map peak is 1.86 Jy/beam. (b) Brightness distribution along the jet, in position angle PA = –30°. The maximum is 1.86 Jy/beam.

temperature of the core is $T_b = 10^{12}$ K. Figure 2.4b presents the brightness distribution along this jet.

Object 1803+784. The 8.4 GHz structure of this BL Lacertae object shows a compact core and a chain of other compact components toward the west (Fig. 2.5.a). This chain of components probably corresponds to fine structure in a jet. In particular, it reflects a spiral structure, indicated by the dashed line. The brightest component is 0.45 mas (1.8 pc) in size, and has a brightness temperature $T_b = 0.13 \times 10^{12}$ K. It is possible that the true core is the weaker component which is located to the east of the brightest component. Its lower brightness may be associated with absorption of the core emission by a surrounding ionized medium, as has been observed for the quasar 3C345 (Matveenko 1993). Figure 2.5b shows the brightness distribution along the jet in PA = –95°.

An overall similar structure, with two components west of the core in position angle PA = –90°, was seen in the earlier 8.4-GHz images of Charlot (1990). These two components are located at distances of 1.3 mas (5.1 pc) and 4 mas (16 pc) from the core. Our data at 13 cm support these results (Fig. 2.5c). The observed structure agrees with the observational data at 1.66 GHz, which show a core and jet extending to 30 mas (120 pc) in position angle PA = –100° (Eckart *et al.* 1987). More complete data have since been obtained by Witzel *et al.* (private communication).

Object 2145+067. The brightness distribution of this blazar at 5 GHz shows a component to the south of the core (Wehrle *et al.* 1992). At 2.3 GHz, an extended component with size 5 mas (21 pc) in position angle PA = 140° can be seen (Britzen 1993). In our image, with resolution 0.25 mas, we distinguish a central bright component and extended emission oriented

along PA = 140° (Fig. 2.6a). The size of the compact core is 0.25 mas, or 1 pc, and its brightness temperature is $T_b = 1.4 \times 10^{12}$ K. A compact component can be seen 1 mas south of the core, as in the image at 6 cm. The brightness distribution along PA = 140° is shown in Fig. 2.6b.

Object 2234+282. This quasar is not resolved at 4.8 and 1.4 GHz (Price *et al.* 1993). Zensus *et al.* (1984) give an upper limit to the size of the unresolved component at 5 GHz of 0.5 mas. In our 8.4-GHz image with resolution 0.33 mas, we observe a jet in position angle

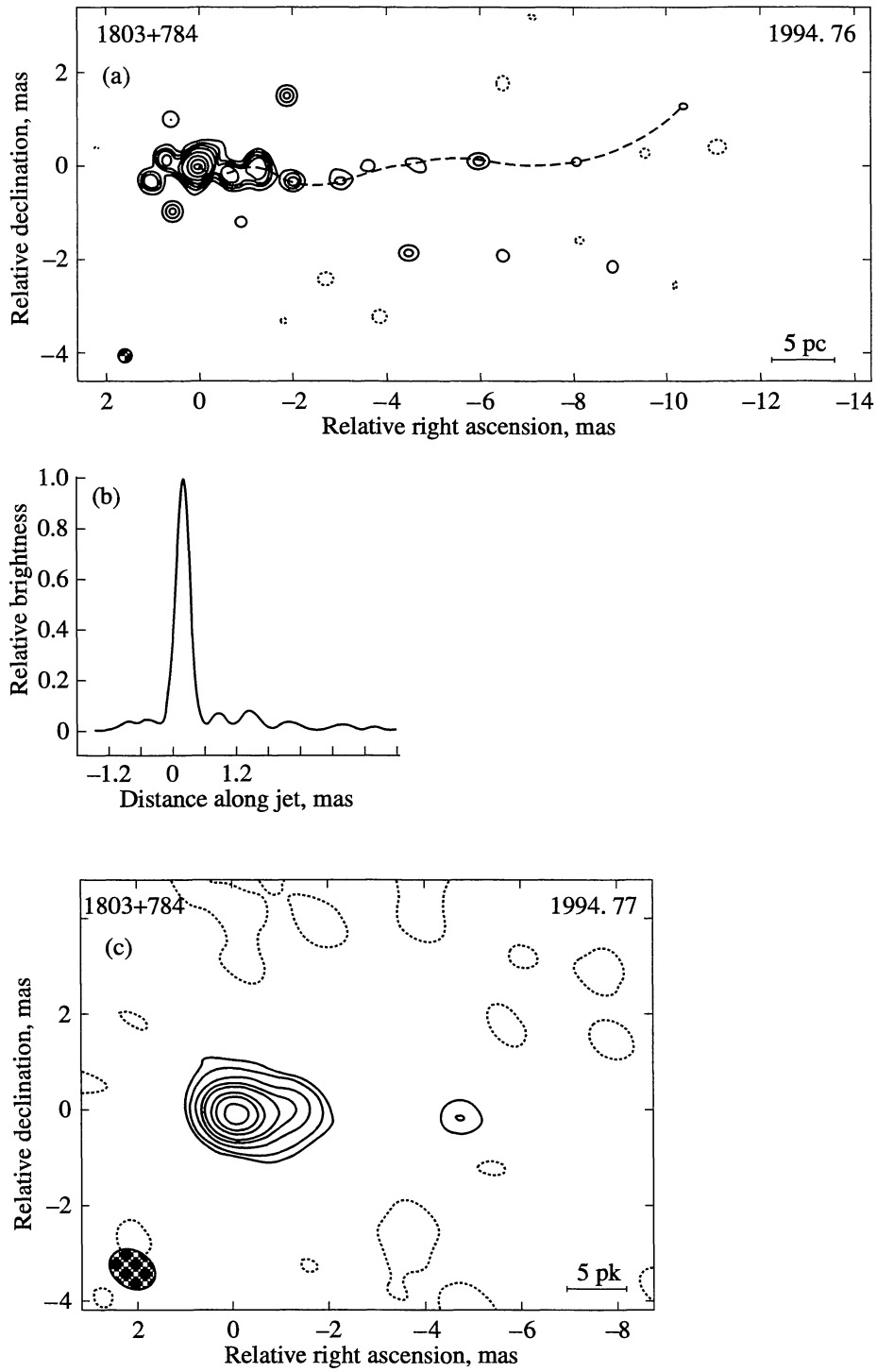

Fig. 2.5. (a) 1803+784. Same as in Fig. 2.1a. The resolution is 0.30 × 0.30 mas, and the map peak is 0.66 Jy/beam. (b) Brightness distribution along the jet, in position angle PA = –90°. The maximum is 0.66 Jy/beam. (c) Brightness distribution at 13 cm.

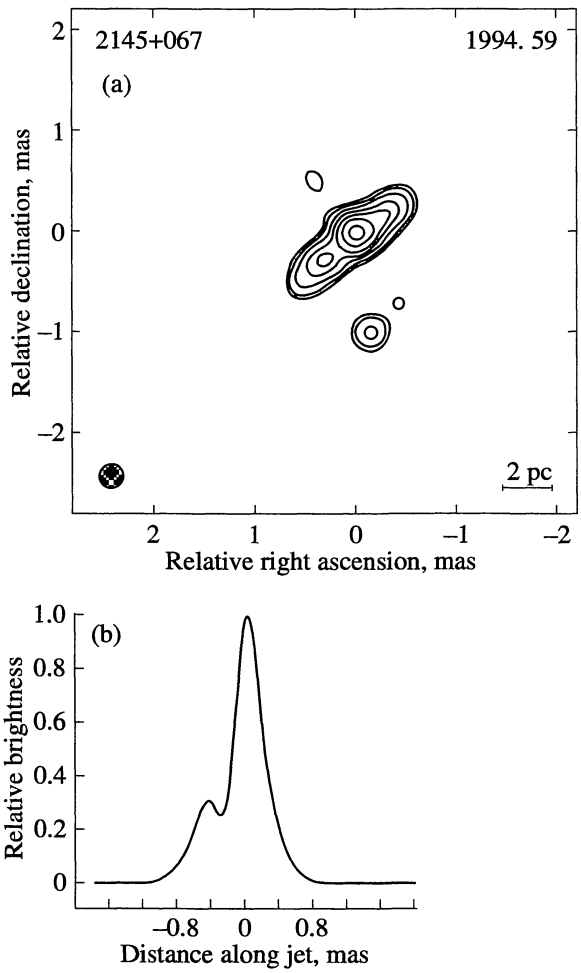

Fig. 2.6. (a) 2145+067. Same as in Fig. 2.1 a. The resolution is 0.25 × 0.25 mas, and the map peak is 3.73 Jy/beam. (b) Brightness distribution along the jet, in position angle PA = 140°. The maximum is 3.73 Jy/beam.

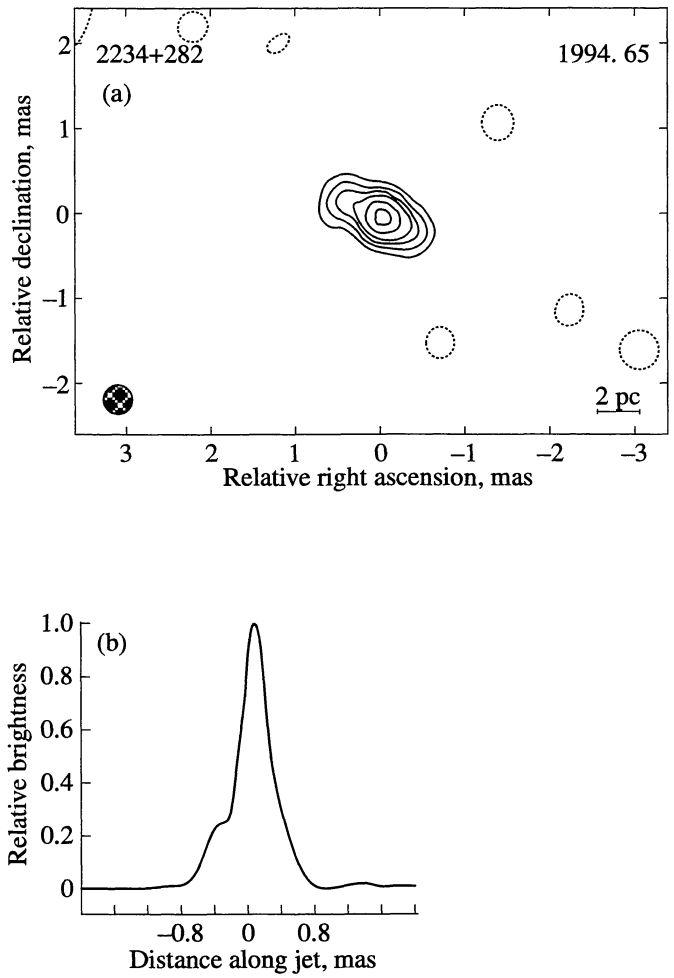

Fig. 2.7. (a) 2234+282. Same as in Fig. 2.1a. The resolution is 0.33 × 0.33 mas, and the map peak is 0.60 Jy/beam. (b) Brightness distribution along the jet, in position angle PA = 60°. The maximum is 0.60 Jy/beam.

PA = 60° (Fig. 2.7.a). The central core is 0.41 mas (1.7 pc) in size, and has brightness temperature T_b = 0.1 × 10^{12} K. The brightness distribution along the jet direction is shown in Fig. 2.7b.

CONCLUSION

We have constructed the brightness distributions for a number of sources with active nuclei—quasars, BL Lacertae objects, and blazars—using 8.4-GHz geodetic VLBI data. The angular resolution provided by these observations is 0.2–0.35 mas, and the resulting dynamic range is 20 dB. Most of the objects have a core–jet structure. The sizes of the cores are between 0.2–0.5 mas, or 0.7–1.8 pc, and their brightness temperatures do not exceed $T_b \leq 10^{12}$ K. We observed symmetrical structure relative to a bright central component in a number of sources. It is possible that this indicates that the core is less bright than the component nearest to it (the central component). The positions of the compact components in 1803+784 suggest that the jet in this source may have a spiral structure. The parsec-scale structure has roughly the same orientation as the structure on larger scales.

ACKNOWLEDGMENTS

We thank the Goddard data analysis center for providing us with the geodetic VLBI data (Helou *et al.* 1991) and D. Shaffer for the SEFD coefficients. We also thank M. Braginskaya and L. Petrov for making it possible for us to use the BORIN astrometric database. This work was supported by the Russian Foundation for Basic Research (project no. 96-02-16367) and the *Astronomy* program (8-232).

REFERENCES

Becker, R.L., White, R.L., and Edwards, A.L., *Astrophys. J., Suppl. Ser.*, 1991, vol. 75, p. 1.

Britzen, S., Diplomarbeit, Universitat Bonn, 1993.

Charlot, P., *Astron. Astrophys.*, 1990, vol. 229, p. 51.

Clark, T.A., Bosworth, J., Vandenberg, N., *et al.*, *Pis'ma Astron. Zh.*, 1995, vol. 21, p. 129.

Eckart, A., Witzel, A., Biermann, P., *et al.*, *Astron. Astrophys., Suppl. Ser.*, 1987, vol. 67, p. 121.

Gabuzda, D.C., Kollgaard, R.I., Roberts, D.H., and Wardle, J.F.C., *Astrophys. J.*, 1993, vol. 410, p. 39.

Helou, G., Madore, B., Schmitz, M., *et al.*, *Databases and On-line Data in Astronomy*, Egret, D. and Albrecht, M., Eds., Dordrecht: Kluwer, 1991, p. 89.

Matveenko, L.I., *Pis'ma Astron. Zh.*, 1993, vol. 19, p. 291.

Matveenko, L.I., Kardashev, N.S., and Sholomitskii, G.B., *Izv. VUZov. Radiofizika*, 1965, vol. 8, p. 651.

Matveenko, L.I., Sagdeev, R.Z., Kostenko, V.I., *et al.*, *Pis'ma Astron. Zh.*, 1983, vol. 9, p. 415.

Pearson, T.J., *Bull. Am. Astron. Soc.*, 1991, vol. 23, p. 991.

Price, R., Gower, C.A., Hutchings, J.B., *et al.*, *Astrophys. J., Suppl. Ser.*, 1993, vol. 86, p. 365.

Schonfelder, V., *Astrophys. J., Suppl. Ser.*, 1994, vol. 92, p. 593.

Shaffer, D.B., Marscher, A.P., Marcaide, J., and Romney, J.D., *Astrophys. J.*, 1987, vol. 314, p. L1.

Wehrle, A.E., Cohen, M.H., Unwin, S.C., *et al.*, *Astrophys. J.*, 1992, vol. 391, p. 589.

Zensus, J.A., Porcas, R.W., and Pauliny-Toth, I.I.K., *Astron. Astrophys.*, 1984, vol. 133, p. 27.

Translated by D. Gabuzda